Tribological characteristics of human vascular smooth muscle cells: the implication of disease state on friction

Emily R Clark [ab], Karen Hemmings [b], Silvia Greco [ab], Anne Neville [a], Karen E Porter [b] and Michael G Bryant [a]*

[a] Institute of Functional Surfaces (iFS), University of Leeds, Woodhouse Lane, Leeds, UK

[b] Leeds Institute for Cardiovascular and Metabolic Medicine (LICAMM), University of Leeds, Woodhouse Lane, Leeds, UK

*Corresponding author. Email: M.G.Bryant@Leeds.ac.uk

Keywords:

Abbreviations: SMC = smooth muscle cell, EC = endothelial cell, FBS = foetal bovine serum, DMEM = Dulbecco's modified Eagle medium

Abstract

The aim of this study was to establish a simple tribological model to assess the frictional properties of non-diabetic (ND) and Type 2 diabetic (T2DM) patients with the view to better understand the interfacial processes off icing in-vivo during angioplasty. Human primary smooth muscle cell (SMC) monolayers from non-diabetic (ND) and Type 2 diabetic (T2DM) patients were isolated and cultured. The coefficient of friction of ND and T2DM SMC monolayers was measured using a micro-tribometer set-up at normal loads (F_n) of 0.4 and 0.8 mN. The coefficient of friction was dependent on load and disease state. The cycle average coefficient of friction of patient grouped SMCs was $\mu = 0.107\pm0.03$ and 0.22 ± 0.01 for ND and T2DM respectively. Within the ND group, the coefficient of friction was seen to be patient specific, with the coefficient of friction varying significantly from $\mu = 0.03\pm0.03$ to 0.185 ± 0.07. Results show that disease state will affect the frictional properties of SMCs. In turn the disease state may also influence the SMCs susceptibly to tribologically induced inflammation.

1. Introduction

The importance of tribology in the human body has long been recognised in terms of the natural bearing surfaces seen in the skeletal joints [1]. However with advancements in modern medicine, for example the development of minimally invasive and precision surgery, surgical robotics and medical devices, interest concerning the links between tribological contacts at soft-tissue interfaces is growing. This is mainly driven through the 1) need to better understand the trauma and adverse remodelling processes which may occur due to mechanical contact and 2) the need for better prediction tools to aid with design and application of future surgical devices or procedures. In light of this, multi-scale test methodologies have been developed to better understand biological processes. These range from macroscopic tissue in-vitro animal models to single cell assessments. Macroscopic tissues are each comprised of specialist cells which contribute to the structure and function of the tissue.

In these applications the interface is not passive. It must be considered as a dynamic and active system in which living cells respond to stimuli in the form of tribological forces via defined biological pathways in addition to the nature of any disease affecting the local properties of the cells or tissue. Cells sense and react to mechanical force signals via a process termed mechano-transduction; this process is involved in physiological mechanisms such as tissue homeostasis [2], wound healing [3] and vessel tone [4] in addition to its implication in various pathological mechanisms such as atherosclerosis [5, 6], osteoporosis [7] and various cardiomyopathies [8]. Especially pertinent to the world of biotribology is the nature of the interface between biomaterials and living tissue in medical devices. Frictional forces at this interface play a central role in device safety and life-span: the function of urethral catheters [9], contact lenses [10], cement for orthopaedic implants [11] are governed by friction at the biomaterial-tissue interface. Characterising the effects of tribological forces on cellular function are commentary to macroscopic tissue samples. Soft tissue trauma / damage via histological techniques is crucial to furthering the understanding of the device-tissue interface. However damage or alterations to cell function is not universally apparent at the tissue level.

The use of cellular monolayers enables the initial bio-chemical processes associated with adverse remodelling of inflammatory processes due to mechanical contact to be determined using conventional biological assays. Furthermore, cells are able to remodel tissue and so damage or undesirable effects may only become noticeable days or even weeks after the cells experience the initial mechanical contact.

Annually, there are 800,000 stents implanted into coronary arteries alone world-wide, with rising numbers due to the global burden of cardiovascular disease and Type 2 diabetes [20]. Despite the latest developments in stent and angioplasty devices, the failure rate for coronary stents is 10% after one year and as high as 30% after one year in peripheral stents due to SMC mediated in-stent restenosis [21, 22]. A schematic of the regions of tribological interactions during angioplasty / stent deployment and arterial anatomy is shown in Figure 1. A principal cell type in blood vessel walls, smooth muscle cells (SMCs) in addition to their primary role of contraction to maintain homeostasis, also play a role in stent failure as mechanical forces induce a switch in cell phenotype and gradually form a neointimal hyperplasia in the lumen of the vessel leading directly to re-occlusion of the artery (in-stent restenosis) [12-17]. Denudation of the endothelium (cellular barrier at the lumen of the vessel) during angioplasty can lead to SMC proliferation and dysfunction in the vessel wall, contributing to adverse remodelling and re-occlusion, albeit the underpinning tribological mechanisms are not well understood [18, 19].

$$\mu = \frac{F_t}{F_n}$$

$$F_t = \tau_i A_r$$
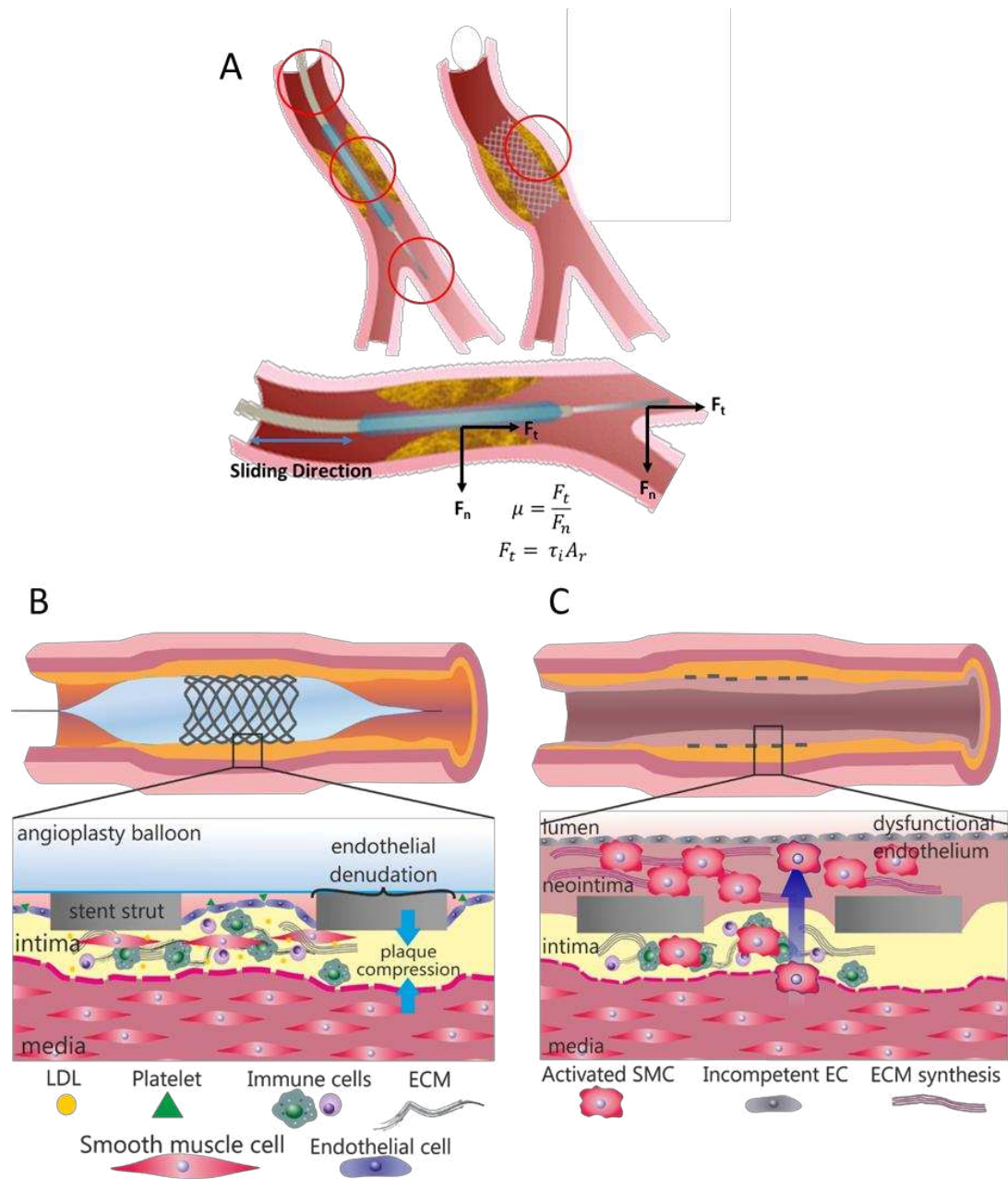
Figure 1. Schematic of A: example of interfaces created during intravascular surgery, B: stent deployment via angioplasty balloon on guidewire and C: formation of neointimal hyperplasia leading to in-stent restenosis with vascular anatomy view. Panel A: The stent is expanded at the target lesion with an angioplasty balloon which is inflated via an endovascular catheter. The artery consists of a single cell layer called the endothelium at the lumen of the artery. The principle component of the vessel is the media, rich with smooth muscle cells (SMCs) and extracellular matrix. During stent deployment the endothelium is denuded, exposing the smooth muscle cells beneath. The atherosclerotic plaque, rich in immune cell infiltration is compressed by both the angioplasty balloon and the struts of the stent. LDL = low density lipoprotein, ECM = extracellular matrix. Panel B: During the lifetime of the stent, SMCs activate and migrate towards the lumen of the artery where they secrete extracellular matrix and contribute to recruitment of pro-inflammatory cells and formation of a neointimal hyperplasia. Once a critical point in growth of the neointimal hyperplasia is reached, in-stent restenosis has occurred and the device has failed. SMC = smooth muscle cell, EC = endothelial cell. Tribological interfaces such as balloon-artery, stent-artery and guidewire-artery in addition to those which arise due to pulsatile flow and stent migration are present during the lifetime of the device.

Further work is needed to understand the effect of tribological interactions during stent deployment on vascular cell response. *In vivo* models in both animals and humans have been used to determine the relationship between the mechanical forces involved in stent deployment and the development of neointimal hyperplasia resulting eventually in restenosis, which will be described herein. The 'aggressiveness' of stent deployment, a parameter developed by Hoffman *et al.* to conflate balloon/artery ratio with inflation pressure, is linked clinically with formation of neointimal hyperplasia [12]. A common cause of restenosis in experimental animal models is oversizing during stent deployment [20, 21]. However, visualisation of microscale device-tissue interactions and study at the cellular level is complex in *in vivo* models and is complicated by cost and ethical considerations. Finite element analysis modelling of stent deployment is able to uncover patient specific stress patterns within the arterial wall and furthermore can link these to neointimal formation in experimental models [22-24]. In such studies, the relationship between mechanical and tribological forces encountered during stent deployment and the biological response at the cellular level has not yet been explored. Finite element techniques have also been widely employed to assess the nature of the mechanical forces the artery is subjected to during angioplasty and stent deployment [25, 26]. Dunn *et al.* first recorded macroscopic friction measurements on bovine endothelial cells (ECs) using low applied normal loads (milliNewton range) and linked tribological phenomena to cellular response [27]. The coefficient of friction was recorded as μ = 0.03 ± 0.02. However, the experimental set up was not optimised for the requirements of living cells; temperature, CO_2 level and nutrients are essential components of cell culture. Dean *et al.* used atomic force microscopy to assess the frictional behaviour of individual rat aortic SMCs (μ = 0.06) but did not link any such measurements to cell response [28].

The principal aim of this study is to evaluate frictional behaviour of primary human SMCs with and without type 2 diabetes from clinically-relevant patients under physiological relevant loads during angioplasty. As part of this, the role of patient disease state (ND or T2DM) will also be assessed. The framework and results presented in this study provide the foundation to enable

the links between tribological forces with cellular response to be determined. Cell viability and adverse vascular cell function in the context of in-stent restenosis will be discussed.

2. Materials and methods

2.1 Isolation of primary cells

Saphenous vein tissue was obtained from patients undergoing coronary artery bypass graft surgery at Leeds General Infirmary, UK. Local ethical committee permission and informed, written patient consent was obtained. The study conformed to the principles outlined in the Declaration of Helsinki. SMC cultures were established from non-diabetic patients (ND) and age-matched patients receiving treatment for Type 2 diabetes (T2DM), by an explant technique described previously [29, 30]. SMCs were maintained in Dulbecco's Modified Eagle Medium (DMEM; Gibco, UK) supplemented with 10% foetal calf serum (Biosera, France), 1% L-Glutamine and 1% penicillin/streptomycin fungizone (both Gibco, UK). SMCs were maintained at 37°C in 5% CO_2 in air and were serially passaged using trypsin/EDTA as necessary. Cells were used for experiments between passages 3 – 4.

2.2 Cell set-up for tribometer

SMCs were seeded at a density of 7.5 x 10^4 in a 6-well polystyrene tissue culture-treated plates and cultured until a single confluent monolayer was formed (just reaching 100% confluency). SMC culture media was supplemented with an additional 1M HEPES in order to maintain physiological pH in the absence of a 5% CO_2 environment during tribometer testing. The whole cell-culture dish was adhered to the base support of the tribometer. Control of the external environment was not possible during tribometer testing. SMCs were exposed to the uncontrolled environment for less than 2 minutes, which is less than routine cell culture within a Class II laminar flow cabinet where SMCs would be exposed to such enviroments. Cells were held in a temperature controlled chamber at 37°C at all other times. Cells were tested three times in three different culture wells for each normal loading regime.

2.3 Tribometer

The tribometer used was an Anton Paar Nano Tribometer (NTR^3, Anton Paar, Graz, Austria), installed with a quad beam cantilever. The tests were performed at two normal loads: 0.4mN and 0.8mN at a sliding distance of 500 µm at a speed of 300 µm/s over 20 cycles in a sinusoidal trajectory, whereby the stage was reciprocated to avoid gross cell removal and match the prior work of Dunn et al [27] for comparison. Both the borosilicate glass probe and the SMC monolayer were fully submerged in cell culture media for the total duration of the experiment (Figure 2). Data was acquired at a rate of 400 Hz. Prior to each test a new probe was used to eliminate any contamination or absorbed protein effects. The cell monolayer was reciprocated against a borosilicate glass hemispherical probe (R = 7.78 mm). Frictional forces (F_t) were resolved under piezo electric control. The effective coefficient of friction of each cycle was determined by taking the averaged magnitude of the friction force within the middle 20% of forward and reverse portions of the sliding cycle. The averaged friction force was then divided through by the averaged normal force at the same cycle point. All data is presented as mean (n > 9 for each patient) ± standard error. Data were found to be normally distributed. Statistical analysis was conducted on all tests which consisted of a two-way ANOVA with a Bonferroni post-hoc test. The friction characteristics of the glass probe reciprocating against a polystyrene tissue culture plate in the absence of cells was recorded to act as a negative control.
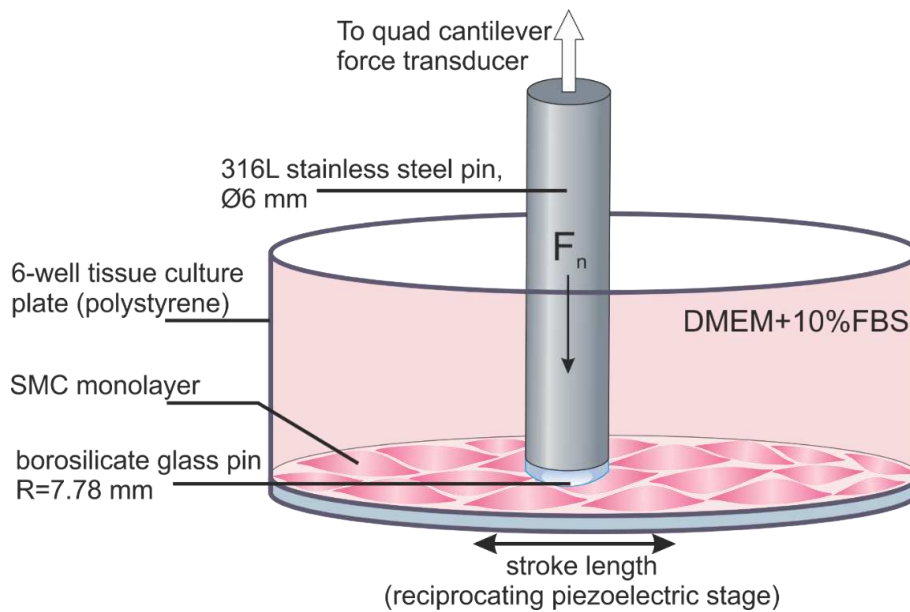
Figure 2. Schematic of tribometer setup for cell friction experiments. DMEM = Dulbecco's modified Eagle medium, FBS = foetal bovine serum, SMC = smooth muscle cell. The piezoelectric controlled stage linearly reciprocated the tissue culture plate containing the SMC monolayer against the glass pin which was held under a constant normal load over a period of 10 cycles. Friction loop data was then captured using the Anton Paar NTR[3]. SMCs were then immediately returned to 37°C once tribological testing had been completed.

2.4   Cell imaging

Following tribological testing, cell detachment was observed using transmission optical microscopy and cell viability was quantified using a fluorescent LIVE/DEAD®viability/cytotoxicity kit (ThermoFisher Scientific, MA, USA). Cell culture medium was removed along with cells which had become detached during testing and washed in 1X phosphate buffered saline (PBS). A staining solution of 2 µM calcein-AM in anhydrous dimethyl sulfoxide (DMSO) and 4 µM ethidium homodimer-1 (EthD-1) in DMSO/H_2O in 1XPBS was then added to each well and left to incubate for 30 minutes at room temperature in the dark. Plates were then imaged under phase and fluorescent red/green using an IncuCyte ZOOM system (Essen BioSciences, MI, USA). Viable cells are able to cleave calcein-AM to produce green fluorescence and EthD-1 is able to enter cells with damaged membranes and produce red fluorescence: live cells are observed as green and dead cells as red. Cell viability was performed via red/green cell counting using image analysis in in-built IncuCyte ZOOM software. A qualitative assessment of viability has been made in this study.

3. Results

3.1 Glass probe vs. tissue culture plate (polystyrene)

Figure 3 shows the frictional data obtained for the glass – culture plate negative control. A gross slip regime was observed at each normal load; there was a well-defined square wave of speed independent friction force. Data was consistent across all loading regimes (Figure 3). Over the loads tested (Range = 0.1 mN to 0.4 mN) there was no significant difference in the mean friction coefficient, $\mu = 0.37 \pm 0.02$ (mean ± standard error, Figure 4).
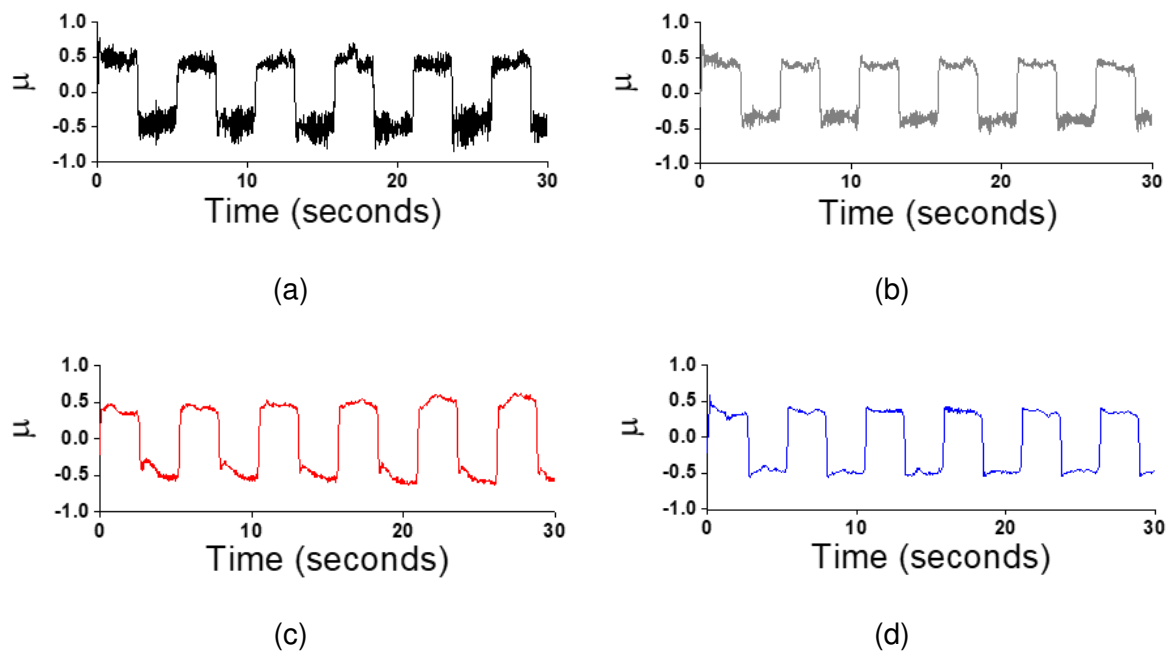
Figure 3. Representative raw friction curves from each normal load: A = 0.1 mN, B = 0.2 mN, C = 0.4 mN, D = 0.8 mN. Three repeats in three different culture plates were conducted at each loading conditions. The glass probe was cleaned prior to testing in each case.
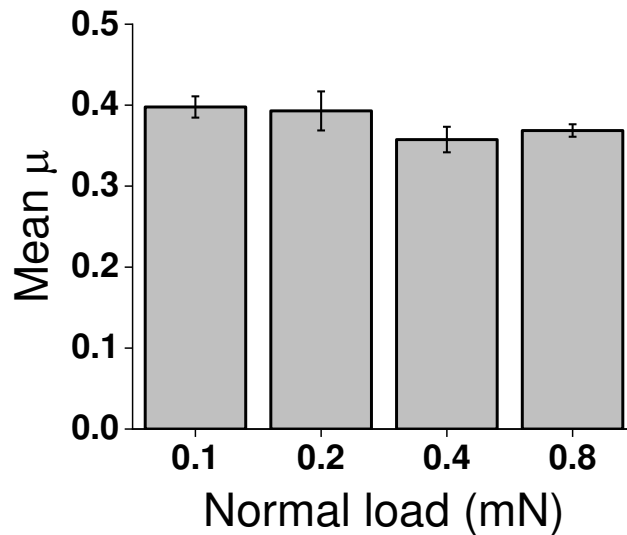
Figure 4. Mean friction coefficient across 10 cycles for borosilicate glass pin reciprocating against tissue culture plate (polystyrene) in the absence of cells. ns = non-significant, one-way ANOVA with post-hoc Tukey test. Data shown as mean ± standard error, (n=3).

3.2 Glass probe vs. SMC monolayer

The frictional characteristics of SMCs from patients with different conditions was evaluated at normal loads of 0.4 mN and 0.8 mN. Testing was completed three times per load per patient on fresh cellular monolayers each time. Representative F_t vs δ profiles for non-diabetic and diabetic patients at 0.4 mN and 0.8 mN are show in Figure 5. Quasi-rectangular shaped F_t vs δ were observed in each case. The magnitude of tangential force was seen to increase with increasing load and between patient conditions.

F_n = 0.4 mN **F_n = 0.8 mN**

(a) (b)

(c) (d)
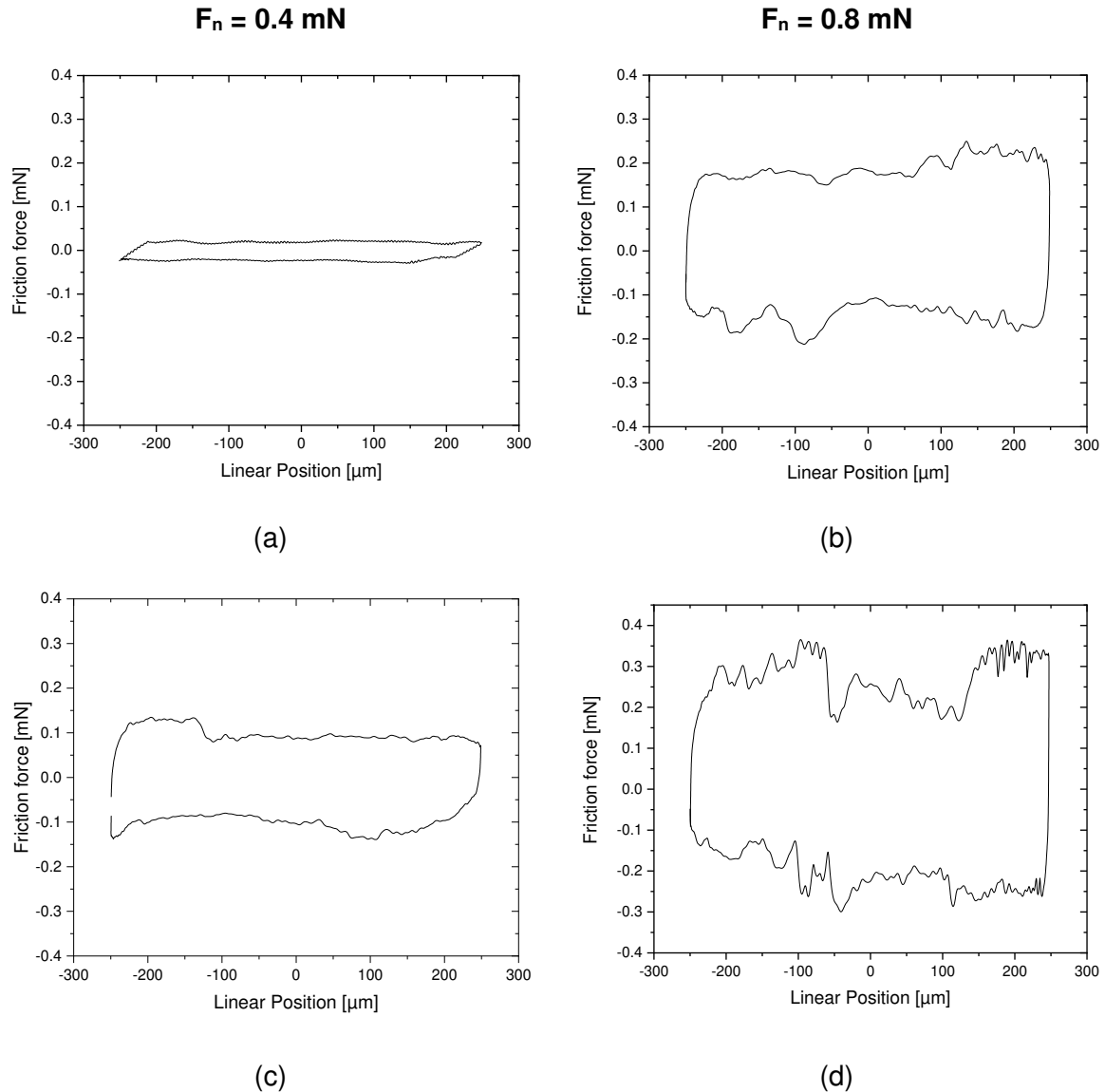
Figure 5. Representative example of F_t vs δ data obtained for borosilicate glass pin reciprocating against tissue culture plate (polystyrene) in the presence of non-diabetic (ND) (a-b) and diabetic (T2DM) (c-d) saphenous vein smooth muscle cells at F_n = 0.4 and 0.8 mN respectively.

The mean coefficient of friction across the 10 cycles is shown in Figure 6 for 0.4 mN and 0.8 mN normal load. For patient grouped ND-SMC monolayers (Figure 6a) the coefficient of friction remained relatively constant throughout the tests although higher at 0.8 mN when compared to 0.4mN. Patient grouped T2DM -SMC monolayers (Figure 6b) showed a similar trend in terms of load. Whilst the coefficient of friction remained relatively stable for ND cells at both normal loads, the coefficient of friction for T2DM -SMC monolayers increased with increasing cycle number (Figure 6c and d). The coefficient of friction differed greatly between

patients but was repeatable and consistent across intrapatient repeats. SMC from individual patients without T2DM displayed coefficients of friction ranging from 0.03±0.02 to 0.41±0.1. This highlights the inherent variability between cell populations independent of diabetic status (Figure 7). Little patient variability was seen for patients with T2DM.
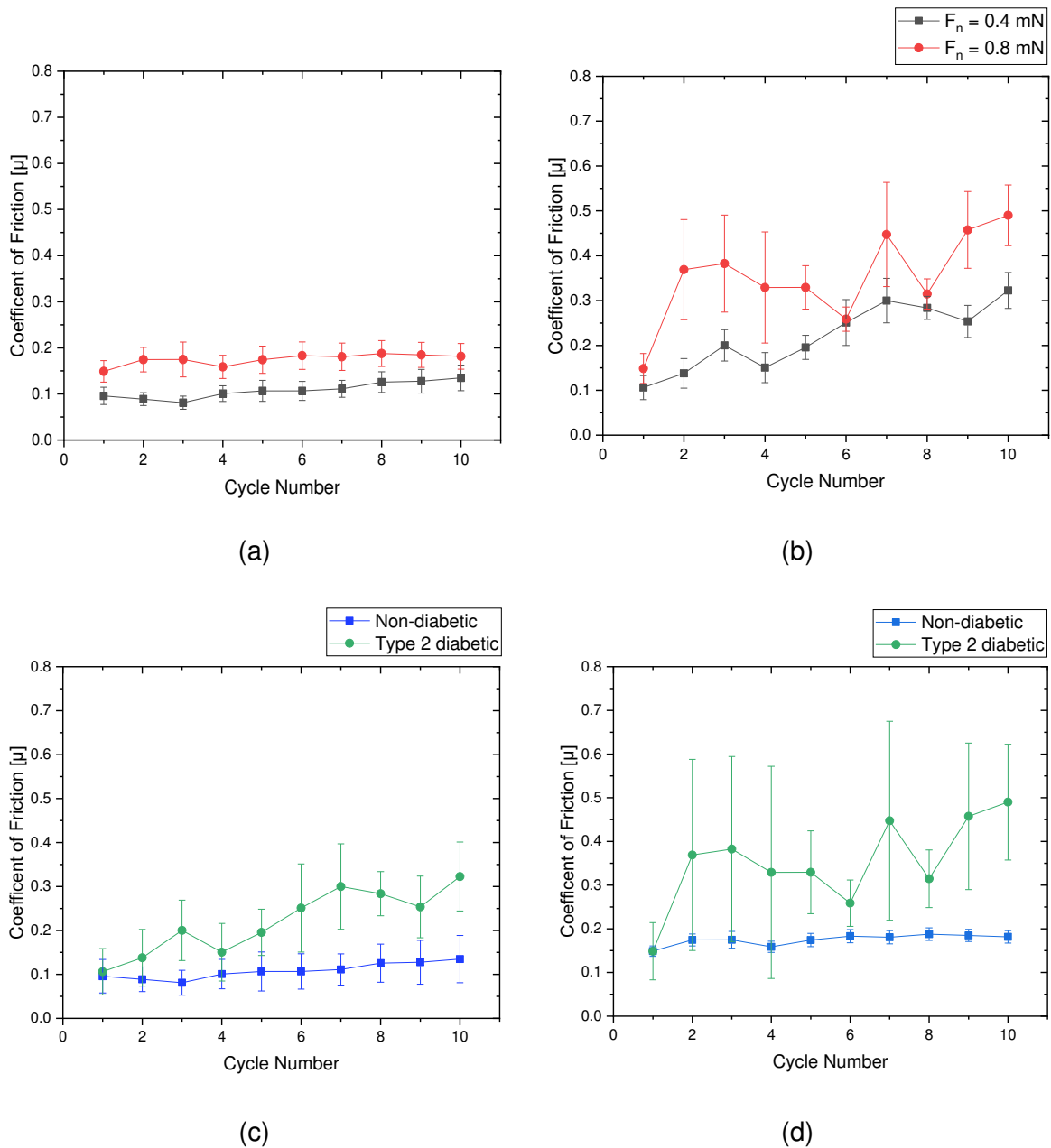
Figure 6. Mean coefficient of friction vs number of cycles for borosilicate glass probe vs. a) ND and b) T2DM SMC monolayers at F_n = 0.4 and 0.8 mN. Figure 7 c and d shows a comparison of the coefficient of friction vs number of cycles for ND and T2DM SMCs at F_n = 0.4 and 0.8 mN, respectively. Data shown are mean ± standard error, coefficient of friction is increased with increased normal load and patient condition.
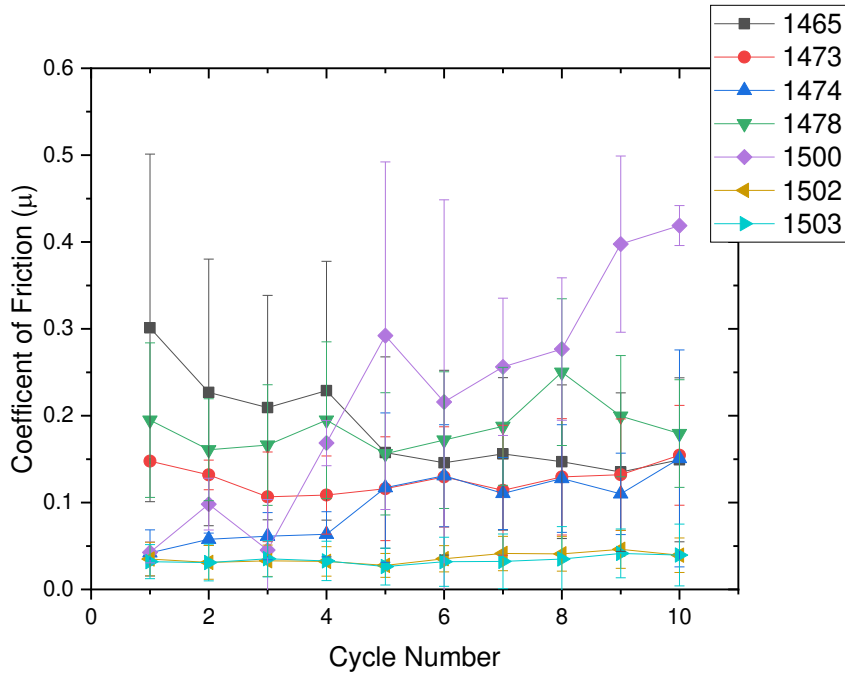
Figure 7. Mean coefficient of friction of borosilicate glass vs ND SMC monolayers. Data shows the mean coefficient of friction for all patients tested.

Figure 8 shows the cycle average coefficient of friction for ND and T2DM SMCs monolayers when slid against a borosilicate glass probe. Increasing the normal load from 0.4 mN to 0.8 mN resulted in a significant increase in the average coefficient of friction across the 10 cycles. For ND cells, the coefficient of friction, μ, was 0.107±0.04 vs. 0.175±0.02 for 0.4 mN and 0.8 mN respectively. For T2DM cells, the coefficient of friction, μ, was 0.22±0.07 vs. 0.35±0.15 for 0.4 mN and 0.8 mN respectively. A significant increase in the coefficient of friction was also seen between ND and T2DM patients. At F_n = 0.4 mN, μ = 0.107±0.04 vs 0.22±0.07 for ND and T2DM respectively. At F_n = 0.8 mN, the coefficient of friction was not significantly different 0.175±0.02 vs 0.35±0.15 for ND and T2DM respectively (two-sample t-test, p<0.001). In all cases, the coefficient of friction for tests with cells was significantly lower than the control samples (Figure 4, p<0.001).
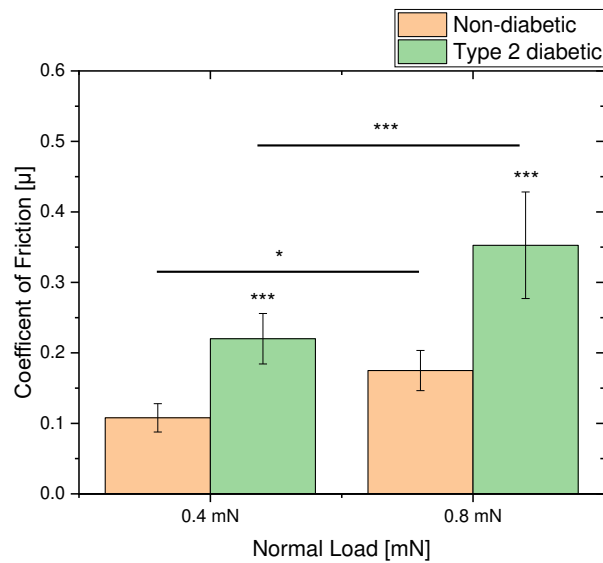
Figure 8. Cycle average coefficient of friction for borosilicate glass probe slid against ND and T2DM SMC monolayers at F_n = 0.4 and 0.8 mN. Data shown are mean ± standard error, ***p<0.001, two way ANOVA and a Bonferroni post-hoc test. A significant increase in the cycle average coefficient of friction was increasing normal load. A significant increase in the cycle average coefficient of friction was also seen at F_n = 0.4 mN between different patient morbidities.

3.3 'Wear scar' visualisation

Figure 9 shows examples of transmission optical microscopy images of the cellular monolayers immediately after tribological assessment. The retention / removal of ND SMC monolayers tested at 0.4 mN was not consistent between patients. Retention and viability of ND SMC monolayers (via Live/Dead) was seen in tests that exhibited low friction (i.e. μ = 0.03±0.03). For ND SMCs that exhibited a higher coefficient of friction (μ ~ 0.1), detachment of SMCs at the outer regions of the sliding area was seen. Within the sliding path retention of SMC derived material was observed (Figure 9e), although the viability of these cells was not maintained as indicated by the Live/Dead analysis. At 0.8 mN complete removal was further confirmed (Figure 9f). Complete removal of SMC after 10 cycles of sliding was observed for all other cases, despite the coefficient of fiction being significantly lower than the cell-free control culture system. Again partial removal of T2DM SMCs were observed at both normal loads tested.

0.4 mN	0.8 mN

(a)　　　　　　　　　　　　　　　　(b)

(c)　　　　　　　　　　　　　　　　(d)

(e)　　　　　　　　　　　　　　　　(f)
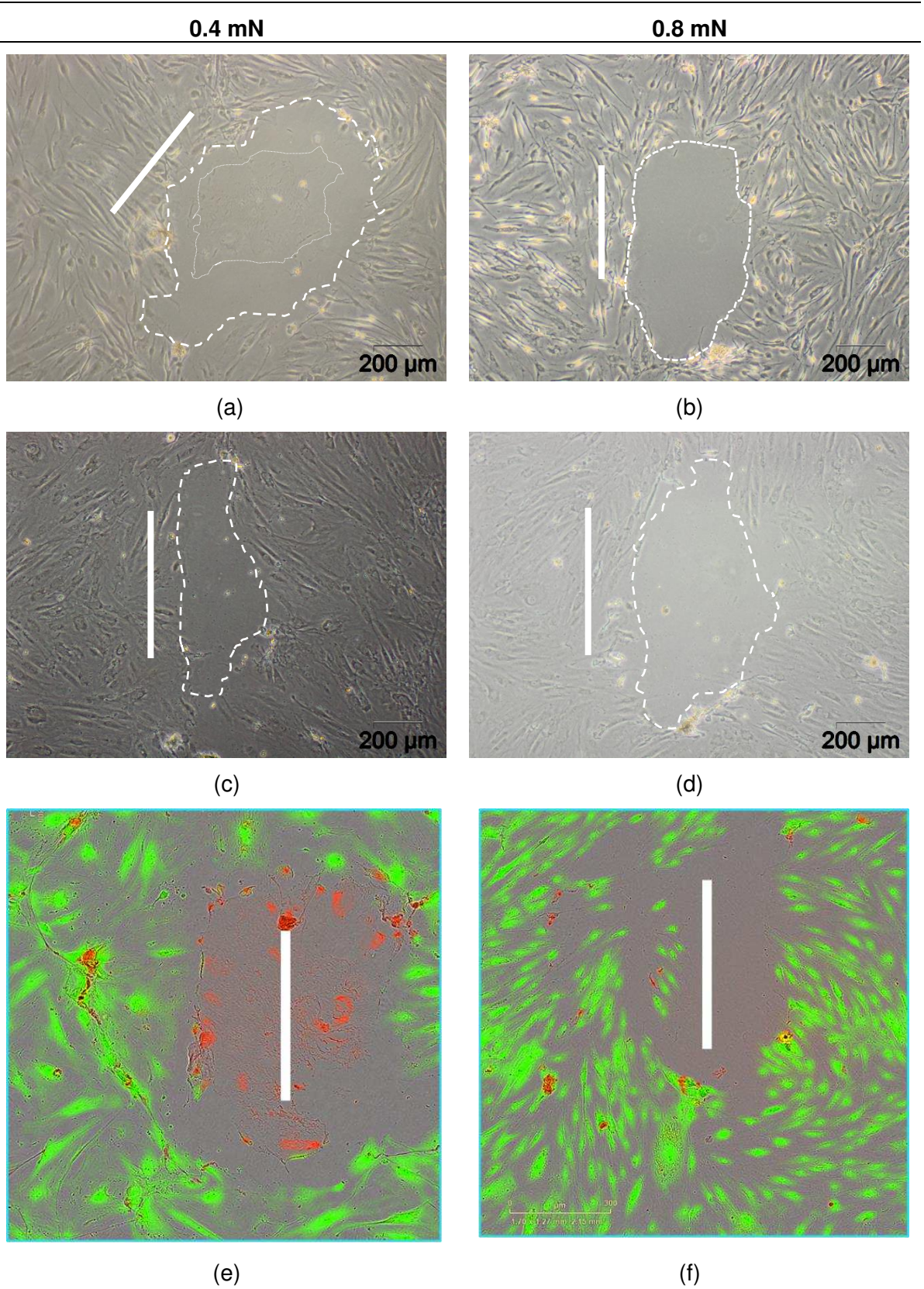
Figure 9. Representative transmission optical microscopy images of for a – b) ND and c-d) T2DMSMC monolayers after 10 cycles of sliding. Figures e-f) show the live/dead staining of the sliding path for non-diabetic SMCs at a normal force of 0.4 and 0.8 mN, respectively. Note the white dash lines represented the boundaries where cellular reattachment / retention were seen. Solid white bar indicated sliding path direction.

4. Discussion

The growing use of intra-vascular procedures to treat cardiovascular disease means in many cases an engineering material will be brought into direct contact with the living biological tissues. As a result mechanical contact at the device – tissue interface will occur resulting in the dissipation of frictional forces, thus energy, at the interface and within sub-surface of the materials. These processes are further complicated by the complex reactive nature of the tissues and cellular components which are known to react to mechanical stimulation, better known as mechano-transduction. Whilst the roles of flow shear stress on vascular cell viability and function have been well studied and characterised [19], the effects of mechanical shear stress are not understood and will manifest themselves at the interface very differently. This is despite the established clinical literature which clearly identifies device – tissues interactions as a pathway to adverse cellular remodelling responses [18, 31]. Furthermore the use of computational based simulation models for device innovation and stratification [17, 23, 24], for example finite element analysis to simulate and quantify shear stresses at soft tissue – device interfaces during angioplasty, often relies on a 'simple' input of friction which is multi-factorial and highly complex.

The implications of tribological stimulation of cellular monolayers has recently been shown by Pitenis et al. [32]. Mechanical shear stresses of 60 Pa are sufficient to initiate the release of pro-inflammatory markers associated with adverse remodelling processes of biological tissues. This study, which has not yet quantified gene expression, does demonstrate the importance of considering the role of patient variability, disease and the altered cell mechanics in the prediction of friction at interfaces. An increase in the coefficient of friction observed in T2DM SMC monolayers will result in an increase in the shear stress experienced by the cells according to $\tau = \mu\sigma$, where $\tau, \sigma \; and \; \mu$ are shear stress, normal stress and the coefficient of friction respectively. This increase in tribological interfacial shear stress will further contribute to the adverse cellular remodelling processes; although the exact molecular pathways are still to be determined and compared against the established literature concerning wall-shear

stresses. This observation and hypothesis correlates with clinical observation where T2DM patients are more susceptible to restenosis after balloon angioplasty when compared to their non-diabetic counterparts.

This study presents initial data concerning the frictional characteristics of human vascular SMC monolayers cultured from patients with and without T2DM. The data presented in this study show that there are significant differences in the frictional characteristics between cell/patient conditions, with patients diagnosed with T2DM displaying higher frictional coefficients. To the author's knowledge, this is the first time that meso-scale frictional coefficients for clinically relevant human primary SMC from patients with and without T2DM have been reported. The average coefficient of friction for patient grouped SMC monolayers was determined as 0.107 ± 0.03 to 0.35 ± 0.01 (mean ± standard error, n = 24) depending upon both the load applied and disease state of the cells. SMCs from individual patients without T2DM displayed coefficients of friction ranging from 0.03 ± 0.03 to 0.185 ± 0.07 with statistical significance seen between patients, highlighting the inherent variability between cell populations independent of diabetic status. Where low values of the coefficient of friction were observed, retention of cellular monolayers was noted and confirmed via optical microscopy and live/dead assays. In some cases where an increased coefficient of friction was observed, non-viable cellular derived materials were observed in the tribological contact area. The variability in coefficient of friction obtained for the T2DM VSMC was not significantly different, although was consistently significantly higher when compared to the ND cells as a group and partial removal of the monolayer after sliding was seen. Dunn *et al.* reported measured friction values of $\mu = 0.03 - 0.06$ for bovine endothelial cells [27]. Rat single cell SMCs are reported to have a frictional coefficient of $\mu = 0.06$ as assessed by lateral force microscopy [28]. Both studies, much like ours, used a borosilicate glass tip for the cell probe and the measurements we report lie within this range giving further confidence to our measurement. The coefficient of friction has also been quantified in the literature for a number of different cell types. Rat SMCs have been measured by lateral force microscopy and the coefficient of friction was

significantly increased to μ = 0.2 when artificially stiffened by cell fixation (by protein cross-linking) [28]. In addition, SMCs have a markedly altered topography in comparison with endothelial cells and have the ability to grow together into a 'pseudo-tissue'. Whilst most studies to date use cell lines that by their very nature are "the same" i.e. homogeneous rather than the accepted heterogeneity that exists both between and within humans, the cells used in this study were isolated from mostly aged human patients who have cardiovascular disease as opposed to cells derived from presumably young animals. The results presented in this study highlight the important role of inter-patient variability and physiological variables such as age, gender, diabetic status, other confounding risk factors and co-existing disease on the tribological characteristics of cellular monolayers.

The biological nature and role in physiology of the cell types are very different and the frictional response of the cells should not be assumed to be similar to cell types published in literature. This is further complicated by the length scale at which the coefficient of friction is measured (i.e. single cell, whole tissue, culture monolayer). Biological mechanisms such as systemic aging and development of cardiovascular disease will affect the structure, function and mechanical properties of SMCs [33, 34]. At the single cell level, Trask and McCallinhart [35] conducted AFM nano-indentation cells on non and T2DM primary VSMCs showing reduced moduli for cells with T2DM (3.60 ± 0.32 kPa vs. T2DM: 2.75 ± 0.22 kPa). It was hypothesised that this reduction in stiffness may be due to underlying alterations in the cytoskeletal arrangement. These observations are supported by Schulze et al [36] who conducted indentation tests using a custom micro-indenter on Madin Darby Canine Kidney cell monolayers treated with and without Blebbistatin (to simulate relaxation in the cell cytoskeleton). The results showed that Blebbistatin-treated cells demonstrated a reduction in contact moduli from 33 to 15.6 kPa when compared to the untreated condition highlighting the importance of cytoskeleton in the cell contact mechanics. However the observation made by Trask and McCallinhart are at odds with whole tissue results. Desyatova et al [37] demonstrated that older age and diabetes mellitus resulted in stiffer and less compliant

tissues. This has also been shown experimentally in rat tissues with experimentally induced diabetes. In the case of diabetes mellitus, elevated glucose levels play an important role in transforming SMCs into osteoblast-like cells with altered cellular phenotype, function, ability to promote calcification and changes in extracellular matrix [38]. Without a doubt the physio-chemical properties of the cells tested will greatly affect the measured coefficients of friction and it is conceivable that the T2DM monolayers tested in this study will have very different time and rate dependant physiochemical properties when compared to the ND cells. The time dependant mechanical properties of the cellular monolayers will influence the evolving contact mechanics effecting the nature of stress distribution within the contact over time. Furthermore the application of tribology will also initiate bio-chemical changes within and at cellular interfaces further influencing the evolving friction and energy dissipation mechanisms. It has been shown by the authors that cells cultured from patients with T2DM are phenotypically distinct from their non-diabetic counterparts. These differences have been documented by us previously [38] and it is likely that these characteristics this could influence their vulnerability from a tribological point of view. Further work to elucidate the links between cell mechanics and tribological properties is to be conducted.

5. Conclusion

From the work presented in this study, the following conclusions can be made:

- The frictional properties of human derived smooth muscle cells with and without T2DM have been measured. The SMCs studied are relevant to patients presenting cardiovascular disease.

- The coefficient of friction for non-diabetic SMCs was comparable to other studies. However this was seen to be patient specific.

- Tribological assessment indicated that the coefficient of friction was higher for T2DM SMC monolayers. This is likely attributed to the difference in physio-chemical properties of the cells which are affected by patient factors such as T2DM.

- The disease state of the SMCs will likely affect the cells susceptibility to tribologically activated adverse remodelling processes.

6. Acknowledgements

7. References

1. Dowson, D. and V. Wright. *Bio-tribology*. in *Proceedings of the Conference on the Rheology of Lubrication, The Institute of Petroleum, The Institution of Mechanical Engineers, and the British Society of Rheology*. 1973. London.

2. Humphrey, J.D., E.R. Dufresne, and M.A. Schwartz, *Mechanotransduction and extracellular matrix homeostasis.* Nat Rev Mol Cell Biol, 2014. **15**(12): p. 802-812.

3. Jiang, M.M., et al., *Changes in tension regulates proliferation and migration of fibroblasts by remodeling expression of ECM proteins.* Experimental and Therapeutic Medicine, 2016. **12**(3): p. 1542-1550.

4. Hill, M.A. and G.A. Meininger, *Arteriolar vascular smooth muscle cells: Mechanotransducers in a complex environment.* International Journal of Biochemistry & Cell Biology, 2012. **44**(9): p. 1505-1510.

5. Haga, J.H., Y.S. Li, and S. Chien, *Molecular basis of the effects of mechanical stretch on vascular smooth muscle cells.* J Biomech, 2007. **40**(5): p. 947-60.

6. Gimbrone, M.A., Jr., et al., *Endothelial dysfunction, hemodynamic forces, and atherogenesis.* Ann N Y Acad Sci, 2000. **902**: p. 230-9; discussion 239-40.

7. Klein-Nulend, J., et al., *Microgravity and bone cell mechanosensitivity.* Adv Space Res, 2003. **32**(8): p. 1551-9.

8.   Lyon, R.C., et al., *Mechanotransduction in Cardiac Hypertrophy and Failure.* Circulation research, 2015. **116**(8): p. 1462-1476.

9.   Dellimore, K.H., A.R. Helyer, and S.E. Franklin, *A scoping review of important urinary catheter induced complications.* Journal of Materials Science: Materials in Medicine, 2013. **24**(8): p. 1825-1835.

10.   Samsom, M., et al., *In vitro friction testing of contact lenses and human ocular tissues: Effect of proteoglycan 4 (PRG4).* Tribology International, 2015. **89**: p. 27-33.

11.   Nich, C., et al., *Macrophages—Key cells in the response to wear debris from joint replacements.* Journal of Biomedical Materials Research Part A, 2013. **101**(10): p. 3033-3045.

12.   Hoffmann, R., et al., *Tissue proliferation within and surrounding Palmaz-Schatz stents is dependent on the aggressiveness of stent implantation technique.* Am J Cardiol, 1999. **83**(8): p. 1170-4.

13.   Cheng, J. and J. Du, *Mechanical stretch simulates proliferation of venous smooth muscle cells through activation of the insulin-like growth factor-1 receptor.* Arterioscler Thromb Vasc Biol, 2007. **27**(8): p. 1744-51.

14.   Qiu, J., et al., *Biomechanical regulation of vascular smooth muscle cell functions: from in vitro to in vivo understanding.* J R Soc Interface, 2014. **11**(90): p. 20130852.

15.   Wentzel, J.J., et al., *Relationship between neointimal thickness and shear stress after Wallstent implantation in human coronary arteries.* Circulation, 2001. **103**(13): p. 1740-5.

16.   Gu, L., et al., *The relation between the arterial stress and restenosis rate after coronary stenting.* Journal of Medical Devices, 2010. **4**(3): p. 031005.

17.   Freeman, J.W., P.B. Snowhill, and J.L. Nosher, *A link between stent radial forces and vascular wall remodeling: the discovery of an optimal stent radial force for minimal vessel restenosis.* Connect Tissue Res, 2010. **51**(4): p. 314-26.

18.   Otsuka, F., et al., *The importance of the endothelium in atherothrombosis and coronary stenting.* Nat Rev Cardiol, 2012. **9**(8): p. 439-53.

19.   Van der Heiden, K., et al., *The effects of stenting on shear stress: relevance to endothelial injury and repair.* Cardiovasc Res, 2013. **99**(2): p. 269-75.

20.   Heldman, A.W., et al., *Paclitaxel Stent Coating Inhibits Neointimal Hyperplasia at 4 Weeks in a Porcine Model of Coronary Restenosis.* Circulation, 2001. **103**(18): p. 2289-2295.

21.   Lowe, H.C., et al., *The porcine coronary model of in-stent restenosis: current status in the era of drug-eluting stents.* Catheter Cardiovasc Interv, 2003. **60**(4): p. 515-23.

22.   Gökgöl, C., N. Diehm, and P. Büchler, *Numerical Modeling of Nitinol Stent Oversizing in Arteries with Clinically Relevant Levels of Peripheral Arterial Disease: The Influence of Plaque Type on the Outcomes of Endovascular Therapy.* Annals of Biomedical Engineering, 2017. **45**(6): p. 1420-1433.

23.   Keller, B.K., et al., *Contribution of Mechanical and Fluid Stresses to the Magnitude of In-stent Restenosis at the Level of Individual Stent Struts.* Cardiovascular Engineering and Technology, 2014. **5**(2): p. 164-175.

24.   Martin, D. and F.J. Boyle, *Computational structural modelling of coronary stent deployment: a review.* Computer Methods in Biomechanics and Biomedical Engineering, 2011. **14**(4): p. 331-348.

25.   Xu, J., et al., *Finite Element Analysis of the Implantation Process of Overlapping Stents.* Journal of Medical Devices, 2017. **11**(2): p. 021010-021010-9.

26.   Martin, D. and F. Boyle, *Finite element analysis of balloon-expandable coronary stent deployment: Influence of angioplasty balloon configuration.* International Journal for Numerical Methods in Biomedical Engineering, 2013. **29**(11): p. 1161-1175.

27.   Dunn, A.C., et al., *Macroscopic Friction Coefficient Measurements on Living Endothelial Cells.* Tribology Letters, 2007. **27**(2): p. 233-238.

28.   Dean, D., et al., *Frictional Behavior of Individual Vascular Smooth Muscle Cells Assessed By Lateral Force Microscopy.* Materials, 2010. **3**(9): p. 4668-4680.

29.   Porter, K.E., et al., *Simvastatin inhibits human saphenous vein neointima formation via inhibition of smooth muscle cell proliferation and migration.* J Vasc Surg, 2002. **36**(1): p. 150-7.

30.   Bauer, C.C., et al., *Modulation of Ca(2+) signalling in human vascular endothelial cells by hydrogen sulfide.* Atherosclerosis, 2010. **209**(2): p. 374-80.

31.   Riches, K., et al., *Exploring smooth muscle phenotype and function in a bioreactor model of abdominal aortic aneurysm.* Journal of Translational Medicine, 2013. **11**(1): p. 208.

32.   Pitenis, A.A., et al., *Friction-Induced Inflammation.* 2018. **66**(3): p. 81.

33.   Monk, B.A. and S.J. George, *The effect of ageing on vascular smooth muscle cell behaviour-A mini-review.* Gerontology, 2015. **61**(5): p. 416-426.

34.   Sehgel, N.L., et al., *Increased vascular smooth muscle cell stiffness: a novel mechanism for aortic stiffness in hypertension.* Am J Physiol Heart Circ Physiol, 2013. **305**(9): p. H1281-7.

35.   Trask, A.J. and P.E. McCallinhart, *Type 2 Diabetic Human Coronary Vascular Smooth Muscle Cells Are Less stiff and Less Adhesive to Fibronectin.* 2019. **33**(1_supplement): p. 512.1-512.1.

36.   Schulze, K.D., et al., *Elastic modulus and hydraulic permeability of MDCK monolayers.* Journal of Biomechanics, 2017. **53**: p. 210-213.

37.   Desyatova, A., J. MacTaggart, and A. Kamenskiy, *Constitutive modeling of human femoropopliteal artery biaxial stiffening due to aging and diabetes.* Acta Biomaterialia, 2017. **64**: p. 50-58.

38.   Riches, K., et al., *Elevated expression levels of miR-143/5 in saphenous vein smooth muscle cells from patients with Type 2 diabetes drive persistent changes in phenotype and function.* Journal of Molecular and Cellular Cardiology, 2014. **74**: p. 240-250.